Fabrication and optical characterization of pedestal micro-structures on DUV210 polymer: waveguides structures towards micro-resonators

Marion Specht, Nolwenn Huby, H Lhermite, R Castro-Beltran, Goulc'Hen Loas, Bruno Bêche

▶ **To cite this version:**

Marion Specht, Nolwenn Huby, H Lhermite, R Castro-Beltran, Goulc'Hen Loas, et al.. Fabrication and optical characterization of pedestal micro-structures on DUV210 polymer: waveguides structures towards micro-resonators. European Physical Journal: Applied Physics, 2015, 71 (1), pp.10501.1-10501-6. 10.1051/epjap/2015150207 . hal-01166476

HAL Id: hal-01166476
https://hal.science/hal-01166476v1

Submitted on 22 Jun 2015

HAL is a multi-disciplinary open access archive for the deposit and dissemination of scientific research documents, whether they are published or not. The documents may come from teaching and research institutions in France or abroad, or from public or private research centers.

L'archive ouverte pluridisciplinaire **HAL**, est destinée au dépôt et à la diffusion de documents scientifiques de niveau recherche, publiés ou non, émanant des établissements d'enseignement et de recherche français ou étrangers, des laboratoires publics ou privés.

Fabrication and optical characterization of pedestal micro-structures on DUV210 polymer: waveguides structures towards micro-resonators

M. Specht[1], N. Huby[1], H. Lhermite[2], R. Castro-Beltran[1], G. Loas[1], B. Bêche[1]

[1] Institut de Physique, Université de Rennes 1, IPR CNRS 6251, 35042 Rennes, France
[2] Institut d'Electronique et de Télécommunications, Université de Rennes 1, IETR CNRS 6164, Rennes, 35042, France

Abstract. The paper presents the global design, fabrication and optical characterizations of pedestal waveguides and 2D microresonators made of DUV210 polymer. These particular geometries are achieved thanks to specific deep-UV lithography procedures allowing sub-lambda development coupled to chemical etching able to shape such pedestal configuration on various optical microstructures. Scanning electron microscopy images have confirmed their features. Moreover, such families of pedestal structures were characterized experimentally, including the optical losses measurements for the waveguides and the optical resonance responses for two kinds of microresonators. Optical studies of single mode propagation losses measurements have been performed by a cut back method leading to values close to 20 dB/cm at a 635 nm wavelength. Additionally, resonant spectral analysis has been performed into pedestal rings and racetracks microresonators with a broadband laser source centered at 795 nm, demonstrating the presence of expected theoretical resonances. Free spectral range values of 2.86 nm and 2.51 nm have been measured for these new designed pedestal resonators on DUV210 related to quality factor values superior to 520 and 610 respectively.

1 Introduction

Integrated optics focuses its interest in new-technology fields due to its potential of low-cost and high-speed integrated circuit. Many materials, organic or not, allow to create a large variety of components according to the fabrication techniques [1]. The ability to shape organic components with sub-wavelength patterns requires adequate procedures developed on various polymers. These procedures are based on different approaches as direct laser writing, press-shape method, mask and UV-photolithography with development or direct photo-inscription [2-5]. Microresonators (MRs) are key components in integrated optics thanks to their properties as filters or various sensors. Whispering Gallery Modes (WGMs) rule such MRs physics. These modes appears near the MRs' surface, when light is confined by total internal reflection. Quantified resonances could be observed when the wavelength of the light coupled into the MRs is an integer multiple of the geometrical perimeter [6, 7].

Polymers present a particular interest in integrated optics due to their wide range of properties like simplified process of fabrication, low-cost fabrication facilities, high transparency above 400 nm, possibility to operate at high frequencies. They also offer many possibilities in designing techniques,

leading to very different geometries [8,9]. The polymer used in this paper is the DUV210, particularly interesting because of its tunable refractive index by controlling the exposure time [10]. The devices presented here are prepared by deep UV lithography [11]. Light confinement is the basic of integrated optics which creates the notion of quantification and eigenvectors called optical modes. Putting optical components on a pedestal provides theoretically a better confinement of the light, due to a higher difference of refractive index between the component and the surrounding environment [12] and can also be useful for specific micro-cantilever photonic elements integrated in acoustic and mechanical sensors or actuators [13, 14] or 2D crystals photonics shaped on suspended membranes [15,16]. Moreover pedestals offer interesting possibilities in integrated optics by improving efficiency of components and offering new geometries for coupling light into MRs [17-19].

In this paper, we present the design, realization and characterization of pedestal DUV210 polymer structures from waveguides to microresonators (MRs). First part is devoted to the global fabrication processes leading to various components as waveguides and MRs on pedestal. Their imaging prove the successful realization concerning the technical protocol. Furthermore this section depicts the two experimental platforms used to characterize all these polymeric micro-optical devices. The optical characterizations and the results devoted to the micro-optical losses measurements as well as the resonance spectral analysis for waveguides and MRs on pedestal are reported in the second part. The conclusions regarding the design and characterization of these structures are sum up at the end of the work.

2 Technical protocol, fabrication and experimental technologies

2.1 Fabrication processes and microscopy imaging

The DUV210 liquid polymer appears to be an interesting and an appropriate candidate for photonic devices fabrication by DUV lithography. This polymer is called chemically amplified resist due to the photo acid generator which is added to the copolymer matrix as described in reference [6]. The optical devices and the investigations presented here are shaped in clean room. Starting from (100) silicon wafers with a 1µm SiO_2 thermal layer, two main steps can be distinguished in the fabrication processes so as to achieve pedestal photonic components on DUV210 polymer: the deep UV lithography and the associated development/softbake processes followed by the chemical etching.

The spin-coating parameters such as speed, acceleration and time are determined by the polymer viscosity and the thickness of the layer aimed in such photonic devices. Table 1 summarized the process steps for single-mode optical microstructures fabrication including pedestal rib waveguides and micro-resonators (MRs). We choose a speed of 900 rpm with an acceleration of 5000 $rpm.s^{-1}$ during 30 seconds, leading to layer-thicknesses ranging between 0.9-1.0 µm. Then a softbake at 140°C during 3 minutes evaporates the solvent and completes the cross-linking. The DUV exposure (HBO 1000W/D, mercury short arc lamp from OSRAM) characterized by a 20 $mJ.cm^{-2}$ at λ_{DUV}=248nm

through the quartz-chromium mask imprints the patterns onto the polymer. A second softbake (1 minute at 120°C) is needed to achieve the specific polymerization reaction induced by the previous exposure, and the chip is dipped in the Microposit MF CD-26 developer during 30 seconds in order to highlight the final optical microstructures. A final softbake at 125°C during 5 hours will ensure better optical and mechanical properties. By using the Buffer HF Improved etchant (Transene), the second main step consists in timing chemical etching process to bring out the pedestal configuration under the waveguides and MRs. Such a solution, containing hydrofluoric acid, attacks the silica without theoretically damaging the optical polymer structures.

As a result, Figure 1 a) b), and c) shows off scanning electron microscopy images (SEM) of various DUV210 pedestal optical structures as rib waveguides, ring and racetrack MRs. All these photonic structures have been heightened after 90 seconds of etching so as to dig and shape pedestal under the devices. On Figure 1 b) and c), ring and racetrack MRs featuring respectively a 15µm-radius and a 30µm-coupling length and a 500 nm-gap between waveguides and MRs. These SEM pictures highlight the used of appropriate set of technical parameters (DUV lithography and chemical etching) for the fabrication of various pedestal DUV210 optical structures with submicrometer resolution.

2.2 Experimental platform description

Two experimental platforms described in the schematic diagram of Figure 2 have been used for the global micro-optical characterizations and studies. The first one is composed of specific optical coupling set-up developed for the measurement of optical losses in the pedestal rib waveguides. This is a totally fibered solution and is dedicated to the cut-back method in integrated optics. A single mode microlensed fiber is connected to the laser source (ThorLabs S1FC635PM, λ_0=635nm) and positioned on nanopiezoelectric manipulators (PI E-563I.3) so as to handle and align it precisely (± 10nm) in the three spatial directions in front of the cleaved face of the pedestal rib waveguide. This experiment allows to inject the light with a highly precision and to excite directly the monomode propagation. Symmetrically, a second microlensed fiber is positioned to collect the light and to direct it to an optical powermeter (Ando AQ 2140) for assessing the optical losses.

The second micro-optical platform is dedicated to the optical spectral analysis, meaning pedestal MRs (Fig. 2). This optical bench is characterized by a free space propagation of the light emitted from a fibered broadband laser source (SLD 331 HP2, λ_0=795 nm, $\Delta\lambda$=40 nm) in order to observe several resonant wavelengths. The polarizer ensures TE polarization at the component's entry and the x40 objective focuses the incident beam into the MRs chip. Fine adjustments are also provided by the nanopiezoelectric positioners related to the sample and the two objectives. The beam at the output of the MRs devices is collected and collimated by a x20 objective and simultaneously monitored with a CCD camera (PulNix CCD camera imaging) and an optical powermeter (Hewlett Packard 8153A) in order to optimize the injection. A beam splitter sends 30% of the light to the CCD so as to visualize

the TE_{00} single mode, while the other 70% are lead via a fiber to an optical spectrum analyzer (OSA Ando AQ-6315E).

3 Integrated optical characterizations, results and discussions

3.1 Single mode propagation and optical losses measurements

The optical losses measurements deliver information on the ability of the structure to confine and propagate the optical mode. In order to evaluate the optical losses by propagation of the single mode into the 2µm-width and straight DUV210 pedestal waveguides, a specific micro-optical bench was designed allowing us to achieve effective injection as depicted in the lower part of Figure 2. Optical losses are performed by the cut-back method which consists in measuring the output power for different lengths by cleaving several times the pedestal waveguide. The input light is injected into the waveguide through its cleaved input face by a singlemode microlensed optical fiber positioned onto nanopiezoelectric manipulators. Then, the output signal and the power are collected by another microlensed optical fiber after propagation into the optical structure and is directly measured by the optical powermeter. In order to have the best statistic possible, the same waveguide is used during the measurements and only the output face is cleaved to have the same injection conditions by a judicious protocol injection at the laser source operating at 635 nm. Considering ΔL the distance between two successive output cleaved faces, the various optical power are expressed by the Beer-Lambert law:

$$10\log(P_j/P_i)=\alpha.\Delta L \qquad (1)$$

where $\Delta L = (L_i - L_j)$ with $L_i > L_j$ is the length difference of the waveguide between two measurements, $P_{i,j}$ the respective output powers measured for respectively L_i and L_j, and α the optical losses (dB/cm). The average propagation losses coefficient α is determined graphically as the slope of the straight line of the experimental data points as presented in Figure 3 where $10.\log(P_j/P_i)$ has been plotted as a function of ΔL. The output power was measured for three different laser powers (1 mA, 1.2 mA and 1.5 mA) and four waveguide lengths (1.30 cm, 0.97 cm, 0.67 cm and 0.44 cm). The α average estimations for single mode propagation were evaluated at 24,5±0.8 $dB.cm^{-1}$, 21.0±0.9 $dB.cm^{-1}$, and 23.1±0.8 $dB.cm^{-1}$ for the set laser power. Optical losses in the range of 20 $dB.cm^{-1}$ for such pedestal configuration are acceptable for these specific ultra-short components as MRs in integrated optics. Indeed these MRs never have an active length higher than 100µm, like is defined by the coupling length imaging in Figure 1.

3.2 Optical resonances, spectral analysis and results

Considering the previous results, a new approach to design and characterize DUV pedestal MRs devices has been developed. As mentioned above, the optical losses are quite acceptable therefore it is relevant to develop and characterize more advanced devices as pedestal MRs shaped as ring and racetrack (Fig. 1) and to study their optical resonances. MRs can localize resonant optical modes called Whispering Gallery modes (WGMs) that are located close to the internal surface. The shape and the size of the MRs govern the resonance condition due to the MR's perimeter which corresponds to the geometrical path the light is following. The perimeter of each MR (ring and racetrack) is easily calculated with all the dimensions specified in Figure 1. In order to measure WGMs resonances, the specific bench described previously in section 2.2 and on the upper part of Figure 2 has been developed. It can be mentioned that the CCD camera helps to verify the continuously single-mode (TE_{00}) propagation during the spectral analysis. The nanopiezoelectric positioners enable to optimize the optical injection and additionally the evanescent coupling between the two pedestal structures waveguide and MR and to maximize the output power so as to obtain measurable optical resonances directly with the optical spectral analyzer (OSA).

The source used for the resonances measurements is a broadband laser, therefore the effective group index n_{eff}^{grp} instead of the refractive index of the materials for the optical resonances linked to each quantified WGMs has to be considered. This effective index takes into account the group velocity v_g of the light wave package, which is also more relevant for a broadband source. Due to the physical principle of the WGMs resonances and the optical properties, these modes occur at regular spectral intervals called the Free Spectral Range (FSR) defined as:

$$FSR = \left(\lambda_0^2 / \left(P.\, n_{eff}^{grp}\right)\right) \quad (2)$$

with λ_0 the excitation laser wavelength in vacuum and P the geometrical perimeter of the MR under test.

The most important optical parameters that describe the behavior of a MR are the Free Spectral Range (FSR), the full width at half maximum (FWHM) $\delta\lambda$ and the quality factor $Q=\lambda_0/\delta\lambda$. Under WGMs configuration, Figure 4 confirms the veracity of these resonances by measuring both optical spectra associated respectively to the ring and racetrack pedestal MRs. It can be noticed that the y-axis on Figures 4 a) and b) represent the real power measured in µW and not a normalized transmission or arbitrary unit. The light-spot intensity at the end of the fiber and before the spectral analyzer is clearly visible and easily detectable with such this highly injection optimization. Such experimental spectral results coupled with the fast Fourier transform (FFT) analysis reveal FSR values of 2.86 nm and 2.51 nm respectively for the ring and the racetrack MRs (Fig. 4). Moreover, the FWHM values of $\delta\lambda$=1.5 nm at λ_0=783 nm for ring pedestal MR and $\delta\lambda$=1.3nm at λ_0=796 nm for racetrack pedestal MR are related to quality factor values superior to 520 and 610 respectively.

Ring shapes present a punctual coupling region whereas the racetrack shapes have an expanded coupling region that favors the evanescent coupling and the WGMs excitation as detected in Figure 4. Moreover, by measuring the FSR in the racetrack spectra, the effective group index value of the DUV 210 organic can be determined, and its value is 1.68 at the 795nm wavelength.

4 Conclusion

The feasibility of simple and coupled processes with deep UV lithography and chemical etching on chemically amplified DUV210 polymer has been demonstrated for a set of rib waveguides/MRs on pedestal configuration for the first time. The clean room protocol with all parameters has been established allowing to shape various ring and racetrack MRs on pedestal, highlighted by SEM imagery. Optical characterization on two experimental benches through losses measurements and spectral analysis has shown the single mode propagative ability of the designed components with losses **around to** 20 $dB.cm^{-1}$ and also the capacity of such pedestal set 'waveguides/MRs structures' to feature an adequate optical evanescent coupling and an excitation of intrinsic quantified WGMs. With the later integrated optical microsystems, resonances with a free spectral range of 2.86 nm and 2.51 nm depending on the geometry of the MRs were achieved. Moreover, due to the length differences of the coupling area, the racetrack shape MRs proved to be more efficient than the ring MRs on the ability to encompass WGMs. The measured FWHM leaded to quality factors better than 500 and 600 for both kinds of pedestal MRs. The measurement of the effective group index delivered values close to 1.68, that is 8% higher than the refractive index of 1.55 for such new polymer DUV210 at 795 nm. The goal of building DUV210 optical components on pedestal configuration from waveguides structures towards MRs has been achieved in a simple and reproducible way.

These specific DUV210 polymer family components are quite easy to produce and they can be implemented for filters or futures optical sensors applications.

References

1. T.M. Benson, S.V. Boriskina, P. Sewell, A. Vukovic, S.C. Greedy, A.I. Nosich, *Micro-optical resonators for microlasers and integrated optoelectronics: Recent advances and future challenges* (*Frontiers in Planar Light Wave Circuit Technology: Design, Simulation and fabrication*, Springer, Netherlands, 2005)

2. D.J. Kang, K. Woo-Soo, B.S. Bae, H.K. Park, B.H. Hung, Appl. Phys. Lett. 87, 221106 (2005)

3. H. Cong, T. Pan, Adv. Funct. Mater. 18, 1912 (2008)

4. P. B. Sahoo, R. Vyas, M. Wadhwa, S. Verma: Bull. Mater. Sci. 25, 553 (2002)

5. C. Delezoide, M. Salsac, J. Lautru, H. Leh, C. Nogues, J. Zyss, M. Buckle, I. Ledoux-Rak, C.T. Nguyen, Photon. Technol. Lett. 24, 270 (2012)

6. L. Collot, V. Lefevre-Seguin, M. Brune, J.M. Raimond, S. Haroche, Europhys. Lett. **23**, 327 (1993)

7. D. Pluchon, N.Huby, L. Frein, A. Moréac, P. Panizza, B. Bêche, Optik **124**, 2085 (2013)

8. T. Grossmann, S. Schleede, M. Hauser, T. Beck, M. Thiel, G. von Freymann, T. Mappes, H. Kalt, Opt. Exp. **19**, 11451 (2011)

9. T. Beck, S. Schloer, T. Grossmann, T. Mappes, H. Kalt, Opt. Exp. **20**, 22012 (2012)

10. D. Duval, H. Lhermite, C. Godet, N. Huby, B. Bêche, J. Opt. **12**, 055501 (2010)

11. Rohm & Haas Electronic Materials 2004
http://hone.mech.columbia.edu/wiki/lib/exe/fetch.php?media=wiki:uv210.pdf

12. T. Begou, B. Bêche, N. Grossard, J. Zyss, A. Goullet, G. Jézéquel, E. Gaviot, J. Opt. A : Pure Appl. Opt. **10**, 055310 (2008)

13. K. Zinoviev, C. Dominguez, J.A. Plaza, V.J. Cadarso Busto, L.M. Lechuga, J. Ligthwave Technol. **24**, 2132 (2006)

14. R. Panergo, C.S. Huang, C.S. Liu, P.G. Reinhall, W.C. Wang, J. Ligthwave Technol. **25**, 850 (2007)

15. S.M.C. Abdulla, L.J. Kauppinen, M. Dijkstra, M.J. de Boer, E. Berenschot, R.M. de Ridder, G.J.M. Krijnen, J. Micromech. Microen. **21**, 125010 (2011)

16. P. Pottier, C. Seassal, X. Letartre, J.L. Leclercq, P. Viktorovitch, D. Cassagne, C. Jouanin, J. Ligthwave Technol. **17**, 2058 (1999)

17. L. Luan, S-Y Cho, N.M Jokerts, in *Proceeding of ECTC '07, Reno, Nevada USA, 2007*, p. 2035

18. Z Sheng, L. Liu, S. He, D. Van Thourhout, R. Baets, in *Proceedings of IEEE Conference on Group IV Photonics, San Francisco, USA, 2009*, p. 122

19. C.Y. Chao, W. Fung, L.J. Guo, J. Quantum Electron. **12**, 134 (2006)

Table captions

Table 1. Serial of process steps for the fabrication of the pedestal photonic structures on DUV210 polymer (v, speed; a, acceleration; t, time; T, temperature; E, exposure dose).

Table 1.

Process steps	**Parameters**
Spin-coating $\begin{pmatrix} v \\ a \\ t \end{pmatrix}$	900 rpm 5000 rpm.s^{-1} 30 s
Softbake (t, T)	3 min at 140°C
Exposure dose (E,t at λ_{DUV} = 248 nm)	20 mJ.cm^{-2} 10 s
Post-exposure softbake (t, T)	1 min at 120°C
Development (product, t)	Microposit MF CD-26 30 s
Final softbake (t, T)	5h at 125°C
Buffer HF Improved (Transene) etching (t)	90 s

Figure captions

Fig. 1. Scanning electron microscopy (SEM) image of (a) a 4 μm-width pedestal rib waveguide on DUV 210 polymer (after processes described in Table 1). SEM images of the MRs photonics structures (b) ring shape MR on pedestal and (c) racetrack MR on pedestal (top-view). Parameters *R*, *L=R* and *g* represent respectively the radius, the coupling length and the gap width for the ring and racetrack MRs.

Fig. 2. Sketch of the micro-optical injection platform characterization used in visible wavelength for respectively the optical losses measurements and the optical resonance into the MRs: Superlum red broadband source (SLD 331 HP2, λ_0=795 nm, $\Delta\lambda$=40 nm), red fiber-coupled laser source (ThorLabs S1FC635PM λ_0=635nm) for losses measurement, optical imaging (PulNix CCD camera) and optical spectral analysis (OSA Ando AQ-6315E).

Fig. 3. Quantity $10\log(P_j/P_i)$ as a function of the length ΔL measured for single mode into such pedestal waveguides. Experimental points are fitted for the three laser intensities (I= 1 mA, 1.2 mA and 1.5 mA) four waveguide lengths (1.30 cm, 0.97 cm, 0.67 cm and 0.44 cm). P_j and P_i represent the output powers measured at lengths L_j and L_i with $L_j<L_i$ and $\Delta L=L_i-L_j$.

Fig. 4. Optical spectral analyses and experimental responses (Superlum red broadband source, λ_0=795 nm) into (a) a ring pedestal MR and (b) a racetrack pedestal MR.

Fig. 1.

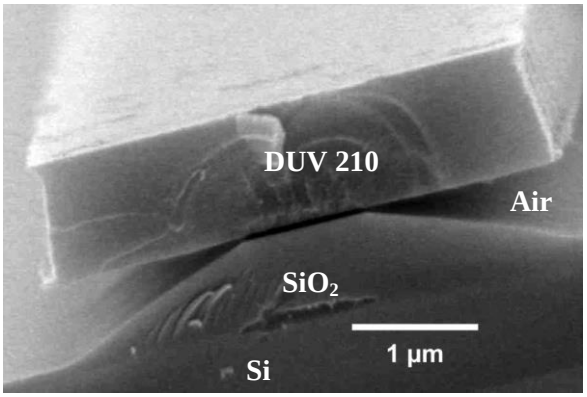
DUV 210
Air
SiO_2
1 µm
Si

(a)

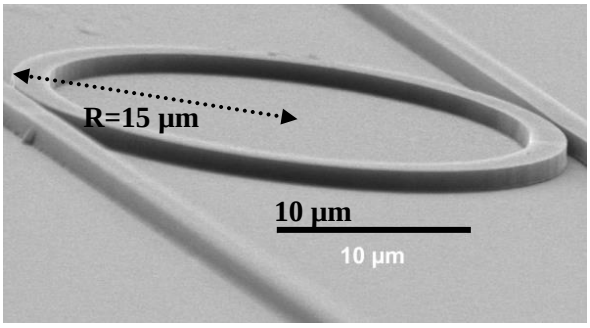
R=15 µm
10 µm
10 µm

(b)

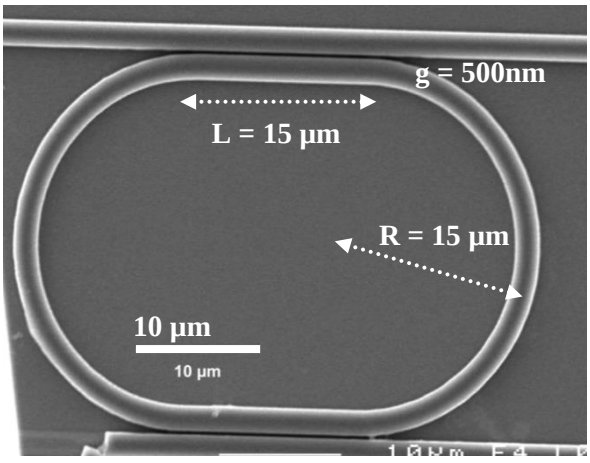
g = 500nm
L = 15 µm
R = 15 µm
10 µm
10 µm

(c)

Fig. 2.

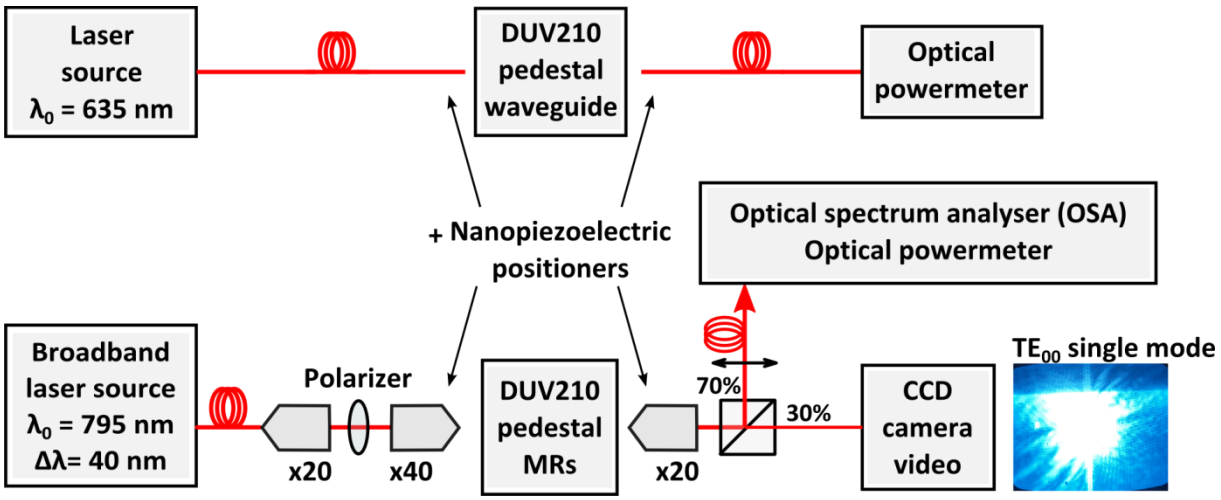
Laser source
λ0 = 635 nm
DUV210 pedestal waveguide
Optical powermeter
+ Nanopiezoelectric positioners
Optical spectrum analyser (OSA)
Optical powermeter
Broadband laser source
λ0 = 795 nm
Δλ= 40 nm
Polarizer
x20
x40
DUV210 pedestal MRs
x20
70%
30%
CCD camera video
TE00 single mode

Fig. 3.

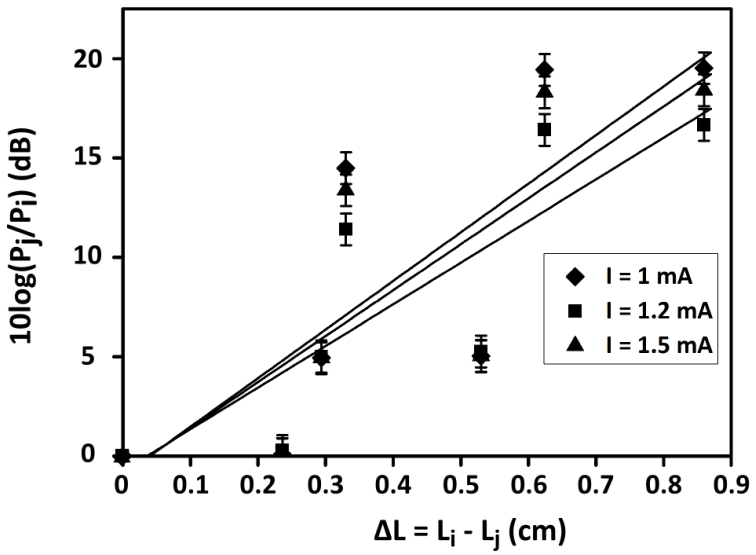
20
15
10
5
0
0
0.1
0.2
0.3
0.4
0.5
0.6
0.7
0.8
0.9
10log(Pj/Pi) (dB)
ΔL = Li - Lj (cm)
I = 1 mA
I = 1.2 mA
I = 1.5 mA

Fig. 4.

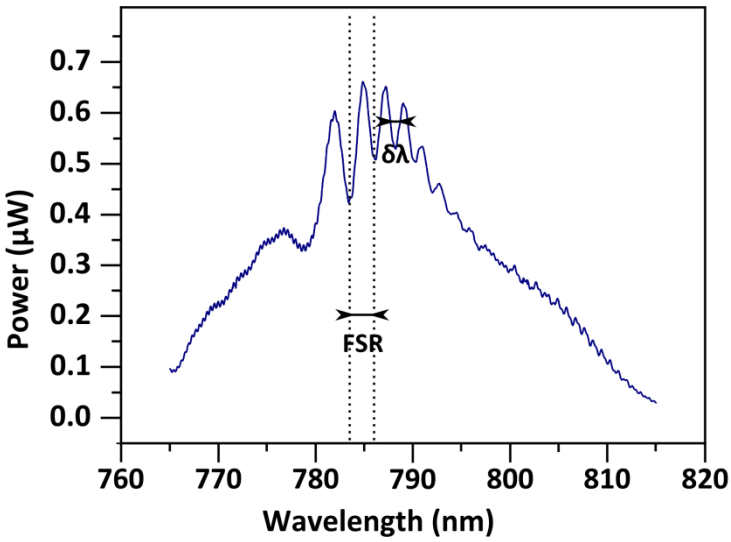
Power (μW)
Wavelength (nm)
δλ
FSR
0.0
0.1
0.2
0.3
0.4
0.5
0.6
0.7
760
770
780
790
800
810
820

(a)

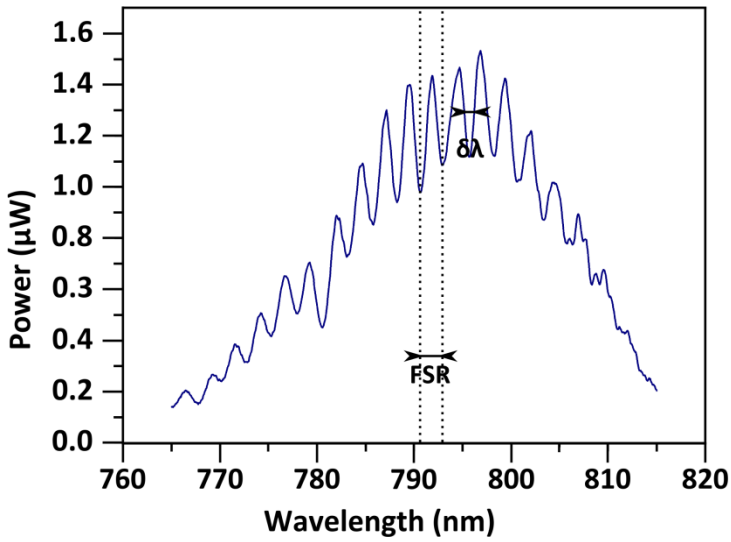
Power (μW)
Wavelength (nm)
δλ
FSR
0.0
0.2
0.3
0.4
0.8
1.0
1.2
1.4
1.6
760
770
780
790
800
810
820

(b)